Acta Cryst E CRYSTALLOGRAPHIC COMMUNICATIONS
ISSN 2056-9890

Crystal structure, Hirshfeld surface analysis and DFT studies of 6-bromo-3-(12-bromododecyl)-2-(4-nitrophenyl)-4*H*-imidazo[4,5-*b*]pyridine

Zainab Jabri,[a] Karim Jarmoni,[a] Tuncer Hökelek,[b] Joel T. Mague,[c] Safia Sabir,[a] Youssef Kandri Rodi[a] and Khalid Misbahi[a]*

[a]Laboratory of Applied Organic Chemistry, Sidi Mohamed Ben Abdellah University, Faculty of Sciences and Techniques, Road Immouzer, BP 2202 Fez, Morocco, [b]Department of Physics, Hacettepe University, 06800 Beytepe, Ankara, Turkey, and [c]Department of Chemistry, Tulane University, New Orleans, LA 70118, USA. *Correspondence e-mail: khalidmisbahifst@gmail.com

Received 6 March 2020
Accepted 13 April 2020

Edited by M. Weil, Vienna University of Technology, Austria

Keywords: crystal structure; imidazole; pyridine; π-stacking; hydrogen bond; disorder.

CCDC reference: 1996788

Supporting information: this article has supporting information at journals.iucr.org/e

The title compound, $C_{24}H_{30}Br_2N_4O_2$, consists of a 2-(4-nitrophenyl)-4*H*-imidazo[4,5-*b*]pyridine entity with a 12-bromododecyl substituent attached to the pyridine N atom. The middle eight-carbon portion of the side chain is planar to within 0.09 (1) Å and makes a dihedral angle of 21.9 (8)° with the mean plane of the imidazolopyridine moiety, giving the molecule a V-shape. In the crystal, the imidazolopyridine units are associated through slipped π–π stacking interactions together with weak C—$H_{Pyr}\cdots O_{Ntr}$ and C—$H_{Brmdcyl}\cdots O_{Ntr}$ (Pyr = pyridine, Ntr = nitro and Brmdcyl = bromododecyl) hydrogen bonds. The 12-bromododecyl chains overlap with each other between the stacks. The terminal –CH_2Br group of the side chain shows disorder over two resolved sites in a 0.902 (3):0.098 (3) ratio. Hirshfeld surface analysis indicates that the most important contributions for the crystal packing are from H···H (48.1%), H···Br/Br···H (15.0%) and H···O/O···H (12.8%) interactions. The optimized molecular structure, using density functional theory at the B3LYP/ 6–311 G(d,p) level, is compared with the experimentally determined structure in the solid state. The HOMO–LUMO behaviour was elucidated to determine the energy gap.

1. Chemical context

Imidazole derivatives are a class of heterocyclic compounds exhibiting pharmacological activities across a wide range of therapeutic targets (El Kazzouli *et al.*, 2011; Martínez-Urbina *et al.*, 2010). Imidazopyridine derivatives are used in medicinal chemistry because of their biological and pharmacological properties, in particular as anti-inflammatory, anti-cancer, antiviral, anti-osteoporotic, anti-parasitic and anti-hypertensive agents. Certain compounds with an imidazopyridine skeleton are used to treat psychiatric and autoimmune disorders (Dymínska, 2015; Bababdani & Mousavi, 2013). They have also been approved as effective antifungal agents and exhibit antimicrobial activities (Devi *et al.*, 2018), some of which can be used for the treatment of disorders characterized by activation of the Wnt signaling pathway (cancer, abnormal cell proliferation, angiogenesis, fibrous disorders, bone or cartilage and arthritis), as well as genetic and neurological diseases. On the other hand, imidazopyridine compounds, which have a specificity to GPR4 as negative allosteric modulators (Tobo *et al.*, 2015), can also be used for the treatment of gastric and/or duodenal ulcers. Several imidazo[4,5-*b*]pyridine derivatives have also been

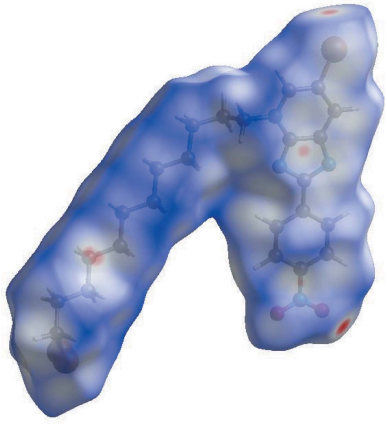

reported as corrosion inhibitors of steel in an acidic environment (Bouayad *et al.*, 2018; Sikine *et al.*, 2016; Yadav *et al.*, 2014), and also as inhibitors of a nanomolar rhodesaine (Ehmke *et al.*, 2013) or the Et-PKG enzyme (Cheng *et al.*, 2010).

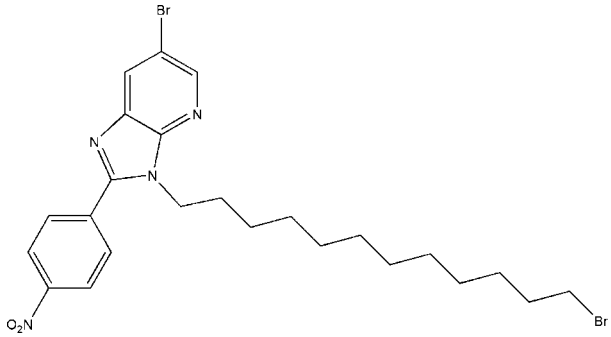

Following our research work directed at obtaining new heterocyclic compounds having an imidazo[4,5-*b*]pyridine moiety, we were interested in the condensation of imidazo[4,5-*b*]pyridine derivatives with di-halogenated chains under phase-transfer catalysis (PTC) conditions. We report herein the synthesis and the molecular and crystal structures of the title compound (I) together with Hirshfeld surface analysis and DFT calculations for comparison with the experimentally determined molecular structure in the solid state.

2. Structural commentary

The molecule of (I) consists of an imidazolopyridine moiety to which a nitrophenyl group is attached to the C atom (C6) of the five-membered ring. The 12-bromododecyl side chain is attached to one of the two N atoms (N1). The imidazolopyridine moiety is planar to within 0.0208 (15) Å (r.m.s. deviation = 0.0122 Å) with atom C3 being the most distant from the least-squares plane. The phenyl ring (C7–C12) is inclined to the above plane by only 1.6 (1)°, making the two ring systems essentially planar. The C4—N1—C13—C14 torsion angle (C13 and C14 are the first two atoms of the 12-bromododecyl chain) is 95.7 (2)°. The C15–C22 portion of the 12-bromododecyl chain is approximately planar [maximum deviation from the least-squares plane running through the eight C atoms is 0.09 (1) Å for C20], and this plane is inclined to that of the imidazolopyridine moiety by 21.9 (8)°, giving the molecule an overall V-shape (Fig. 1). The terminal C24—Br2 portion of the 12-bromododecyl chain is disordered over two resolved sites in a refined ratio of 0.902 (3):0.098 (3).

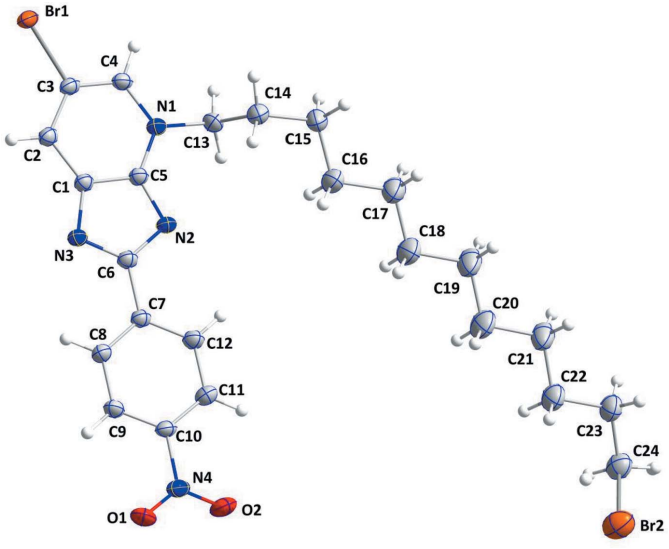

Figure 1
The asymmetric unit of (I) with the atom-numbering scheme. Displacement ellipsoids are drawn at the 50% probability level. Only the major part of the disordered $-CH_2Br$ group is shown.

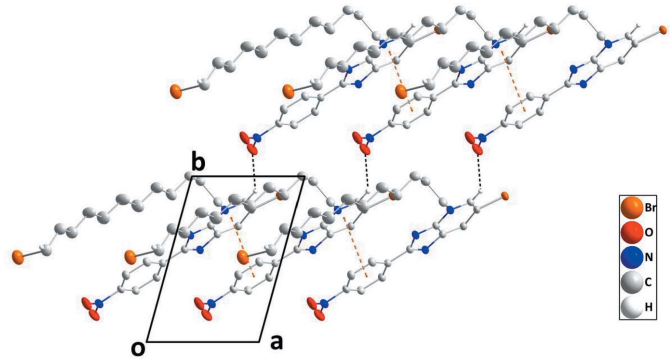

Figure 2
Detail of the intermolecular interactions viewed along the *c*-axis direction. The weak $C-H_{Pyr}\cdots O_{Ntr}$ and $C-H_{Brmdcyl}\cdots O_{Ntr}$ (Pyr = pyridine, Ntr = nitro and Brmdcyl = bromododecyl) hydrogen bonds and π–π stacking interactions are depicted, respectively, by black and orange dashed lines.

3. Supramolecular features

In the crystal, sloped stacks of molecules extending along the *a*-axis direction are formed by slipped π–π stacking interactions between the N1/C1–C5 and C7–C12 rings, with a centroid-to-centroid distance of 3.5308 (13) Å, a dihedral angle of 1.83 (9)° and a slippage of 1.192 Å. The angle between the plane defined by the relevant centroids in the stack and (001) is 19.210 (11)°. The stacks are connected by weak $C-H_{Pyr}\cdots O_{Ntr}$ (Pyr = pyridine and Ntr = nitro) hydrogen bonds (Table 1, Fig. 2). Additional linkage is accomplished by $C-H_{Brmdcyl}\cdots O_{Ntr}$ (Brmdcyl = bromododecyl) hydrogen bonds that influence the arrangement of

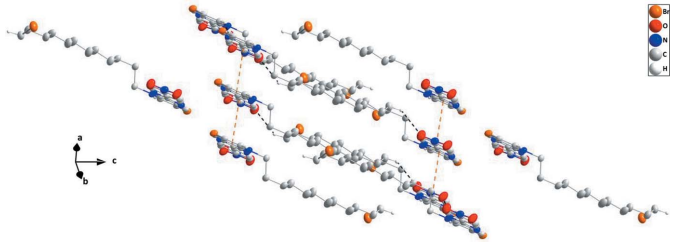

Figure 3
A partial packing diagram projected onto (581) with intermolecular interactions depicted as in Fig. 2.

Table 1
Hydrogen-bond geometry (Å, °).

D—H···A	D—H	H···A	D···A	D—H···A
C4—H4···O1^{i}	0.95	2.43	3.171 (3)	135
C24—H24A···O2^{ii}	0.99	2.53	3.372 (3)	142

Symmetry codes: (i) $x+1, y+1, z$; (ii) $-x, -y+1, -z+1$.

the 12-bromododecyl chains between adjacent stacks (Table 1, Fig. 3).

4. Hirshfeld surface analysis

In order to quantify and visualize the intermolecular interactions in the crystal of (I), a Hirshfeld surface (HS) analysis (Hirshfeld, 1977; Spackman & Jayatilaka, 2009) was carried out by using *Crystal Explorer 17.5* (Turner *et al.*, 2017). In the HS plotted over d_{norm} (Fig. 4), the white surface indicates contacts with distances equal to the sum of van der Waals radii, and the red and blue colours indicate distances shorter (in close contact) or longer (distant contact) than the van der Waals radii, respectively (Venkatesan *et al.*, 2016). The overall two-dimensional fingerprint plot, Fig. 5*a*, and those delineated into H···H, H···Br/Br···H, H···O/O···H, H···C/C···H, H···N/N···H, C···C, C···Br/Br···C and C···N/N···C contacts (McKinnon *et al.*, 2007) are illustrated in Fig. 5*b*–*i*, respectively, together with their relative contributions to the HS. The large number of these contacts suggests that van der Waals interactions and hydrogen bonding play the major roles in the crystal packing (Hathwar *et al.*, 2015). The most important interaction is H···H contributing 48.1% to the overall crystal packing, Fig. 5*b*, followed by H···Br/Br···H, Fig. 5*c*, contacts at 15.0%, H···O/O···H, Fig. 5*d*, contacts at 12.8%, H···C/C···H, Fig. 5*e*, contacts at 6.0%, H···/N···H, Fig. 5*f*, contacts at 5.8%, C···C, Fig. 5*g* contacts at 3.7%, C···Br/Br···C, Fig. 5*h*, contacts at 3.5%, and C···N/N···C, Fig. 5*i*, contacts at 1.6%.

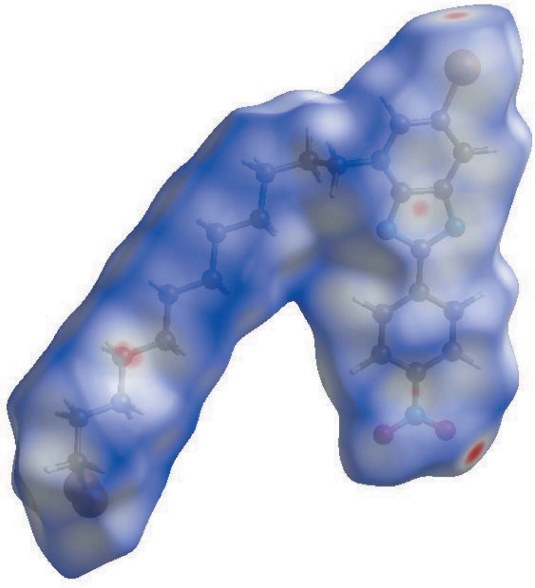

Figure 4
View of the three-dimensional Hirshfeld surface of the title compound plotted over d_{norm} in the range −0.1956 to 1.3971 a.u..

Table 2
Comparison of selected (X-ray and DFT) geometric data (Å, °) for (I).

Bonds/angles	X-ray	B3LYP/6–311G(d,p)
Br1—C1	1.8954 (19)	1.94573
Br2—C24	1.953 (3)	2.02642
O1—N4	1.224 (2)	1.28476
O2—N4	1.233 (2)	1.28545
N1—C5	1.357 (2)	1.36426
N1—C4	1.361 (2)	1.42977
N1—C13	1.473 (3)	1.47563
N2—C5	1.336 (2)	1.35689
N2—C6	1.372 (3)	1.40945
N3—C6	1.346 (2)	1.40939
N3—C1	1.372 (2)	1.38222
N4—C10	1.465 (2)	1.42118
C5—N1—C4	118.57 (17)	117.37
C5—N1—C13	119.67 (16)	119.58
C4—N1—C13	121.75 (17)	120.96
C5—N2—C6	100.79 (16)	101.37
C6—N3—C1	102.17 (16)	101.96
O1—N4—O2	123.30 (19)	122.47
O1—N4—C10	118.48 (18)	118.78
O2—N4—C10	118.22 (18)	118.74
N3—C1—C2	132.04 (18)	133.14
N3—C1—C5	107.59 (16)	105.38
C2—C1—C5	120.37 (18)	121.46

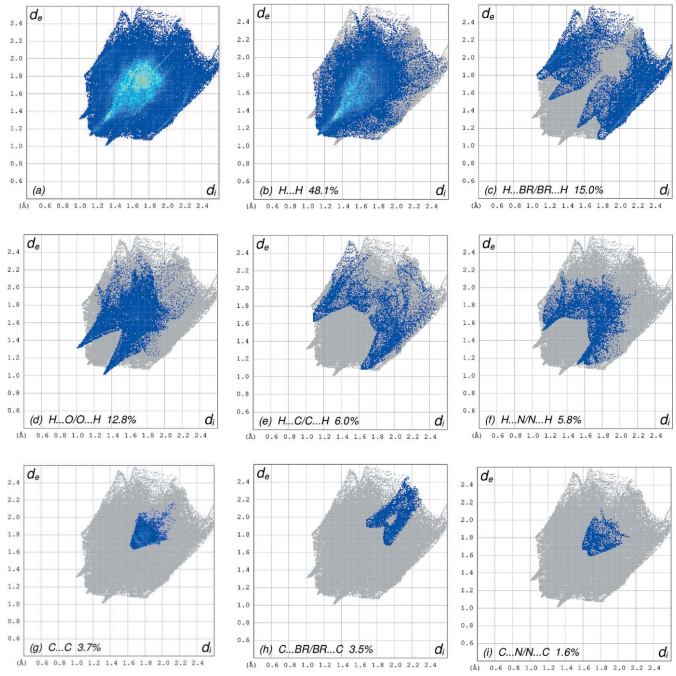

Figure 5
Two-dimensional fingerprint plots for (I), showing (*a*) all interactions, and delineated into (*b*) H···H, (*c*) H···Br/Br···H, (*d*) H···O/O···H, (*e*) H···C/C···H, (*f*) H ···N/N···H, (*g*) C···C, (*h*) C···Br/Br···C and (i) C···N/N···C interactions. The d_i and d_e values are the closest internal and external distances (in Å) from given points on the Hirshfeld surface contacts.

Table 3
Calculated molecular energies for (I).

Total Energy, *TE* (eV)	−175539.349
E_{HOMO} (eV)	−4.0238
E_{LUMO} (eV)	−2.3507
Gap, ΔE (eV)	1.6731
Dipole moment, μ (Debye)	15.7142
Ionization potential, *I* (eV)	4.0238
Electron affinity, *A*	2.3507
Electronegativity, χ	3.1872
Hardness, η	0.8366
Electrophilicity index, ω	3.0715
Softness, σ	1.1954
Fraction of electron transferred, ΔN	2.2788

5. DFT calculations

The optimized structure of the molecule in the gas phase was calculated *via* density functional theory (DFT) using the standard B3LYP functional and 6–311G(d,p) basis-set calculations (Becke, 1993) as implemented in *GAUSSIAN 09* (Frisch *et al.*, 2009). The theoretical and experimental bond lengths and angles are in good agreement (Table 2). Results for E_{HOMO} and E_{LUMO} energies, electronegativity (χ), hardness (η), potential (μ), electrophilicity (ω) and softness (σ) are collated in Table 3. The electron transition from the HOMO to the LUMO energy level is shown in Fig. 6. The energy band gap [$\Delta E = E_{LUMO} - E_{HOMO}$] of the molecule is 1.6731 eV, and the calculated frontier molecular orbital energies, E_{HOMO} and E_{LUMO}, are −4.0238 and −2.3507 eV, respectively.

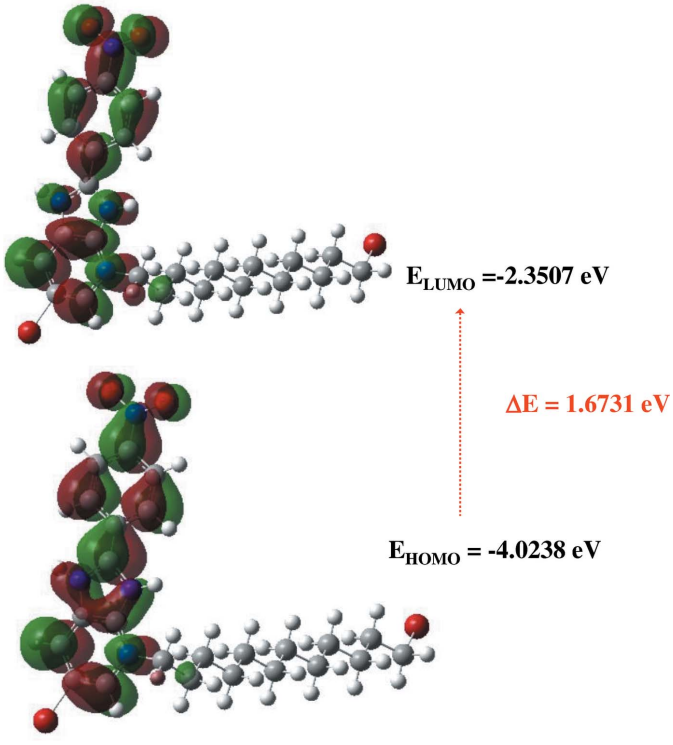

Figure 6
Shapes of HOMO and LUMO of (I) and the energy band gap between them.

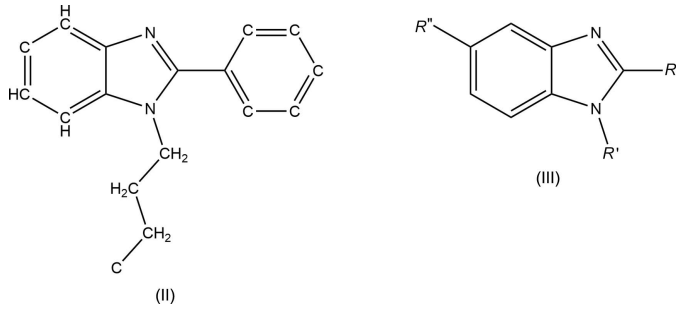

Figure 7
Lewis structures of fragments (II) and (III) used in the database search.

6. Database survey

The importance of benzimidazole derivatives is highlighted by a search of the Cambridge Structural Database (CSD, updated to November 2019; Groom *et al.*, 2016) using a fragment allowing for substituents at the 6-position and having a single carbon atom at the 3- and 4-positions, which resulted in over 1900 hits. Restricting the search to exclude metal complexes and using the fragment (II) (Fig. 7) yielded eight hits most comparable to (I). These are of the general type (III) (Fig. 7) with R'' = H, R = 4-[$Ph_2C{=}C(Ph)$]C_6H_4, R' = *n*-Bu (VEDKEX; Zhang *et al.*, 2018), *n*-hexyl (VEDHUK; Zhang *et al.*, 2018) and R' = 6-(9*H*-carbazol-9-yl)hexyl, R = Ph (DUKJAV; Zhao *et al.*, 2009). Additional ones have R'' = COOMe, R' = *n*-Bu, R = 3,4-$Cl_2C_6H_3$ (ABEJAT; Arslan *et al.*, 2004), 2-[2-(cinnamylthio)benzo[*d*]oxazol-5-yl (TAPVIR; Chanda *et al.*, 2012), and the set is completed by those with R' = *n*-Bu, R'' = CN, R = 3-ClC_6H_4 (WEWVIE; Kazak *et al.*, 2006) or R= 3,4-$(MeO)_2C_6H_3$ (WEWVOK; Kazak *et al.*, 2006) and R'' = NO_2, R' = *n*-Bu, R = 2-(*p*TosNH)C_6H_4 (BUXDUV; Burlov *et al.*, 2016). In all of the matches where R' is an alkyl chain, the base of the chain is approximately perpendicular to the benzimidazole plane but not all of them have the remainder of the chain in a fully extended conformation and in no instances are structures seen in which the alkyl chains overlap. Part of the reason is that the butyl group is not long enough to counteract the packing interactions involving the benzimidazole moiety and the substituents in the 2-position. The possible exception is in DUKJAV where π–π stacking interactions appear to occur between the benzimidazole units and between the carbazole units. Also, all of the related molecules identified have a dihedral angle between the plane of the benzimidazole unit and the plane of the aromatic ring in the 2-position of 28–48° while in (I) the two are nearly coplanar [1.6 (1)°]. This is likely due to packing considerations.

7. Synthesis and crystallization

To a solution of 6-bromo-2-(4′-nitrophenyl)-3*H*-imidazo[4,5-*b*]pyridine (0.4 g, 1.25 mmol), potassium carbonate (2.2 equivalents; 0.38 g, 2.75 mmol) and tetra-*n*-butylammonium bromide (0.2 equivalents; 0.061 g, 0.187 mmo)l in 40 ml of DMF were added in small portions to 1.5 equivalents of 1,12-

Table 4
Experimental details.

Crystal data	
Chemical formula	$C_{24}H_{30}Br_2N_4O_2$
M_r	566.34
Crystal system, space group	Triclinic, $P\overline{1}$
Temperature (K)	150
a, b, c (Å)	6.3291 (11), 9.8911 (17), 21.133 (4)
α, β, γ (°)	76.480 (2), 84.965 (3), 73.891 (2)
V (Å^3)	1235.4 (4)
Z	2
Radiation type	Mo $K\alpha$
μ (mm^{-1})	3.31
Crystal size (mm)	0.48 × 0.23 × 0.20
Data collection	
Diffractometer	Bruker SMART APEX CCD
Absorption correction	Multi-scan (*SADABS*; Krause *et al.*, 2015)
T_{min}, T_{max}	0.23, 0.56
No. of measured, independent and observed [$I > 2\sigma(I)$] reflections	24139, 6598, 5337
R_{int}	0.040
(sin $\theta/\lambda)_{max}$ (Å^{-1})	0.688
Refinement	
$R[F^2 > 2\sigma(F^2)]$, $wR(F^2)$, S	0.035, 0.095, 1.03
No. of reflections	6598
No. of parameters	293
H-atom treatment	H-atom parameters constrained
$\Delta\rho_{max}$, $\Delta\rho_{min}$ (e Å^{-3})	0.72, −0.80

Computer programs: *APEX3* and *SAINT* (Bruker, 2016), *SHELXT* (Sheldrick, 2015*a*), *SHELXL2018/1* (Sheldrick, 2015*b*), *DIAMOND* (Brandenburg & Putz, 2012) and *publCIF* (Westrip, 2010).

dibromododecane. The resulting mixture was stirred magnetically at room temperature for 48 h. After removal of the salts and evaporation of DMF under reduced pressure, the product was separated by chromatography on a column of silica gel using a mixture of hexane/dichloromethane: 1/4 (*v*/*v*) as the mobile phase. Orange single crystals suitable for X-ray diffraction were obtained by slow evaporation of the eluant.

8. Refinement

Crystal, data collection and refinement details are presented in Table 4. Hydrogen atoms were included as riding contributions in idealized positions with isotropic displacement parameters tied to those of the attached atoms. The terminal C24—Br2 portion of the 12-bromododecyl chain is disordered over two resolved sites in a 0.902 (3)/0.098 (3) ratio. The two components of the disorder were refined with restraints so that their bond lengths and angles are comparable.

Funding information

JTM thanks Tulane University for support of the Tulane Crystallography Laboratory. TH is grateful to Hacettepe University Scientific Research Project Unit (grant No. 013 D04 602 004).

References

Arslan, B., Kazak, C., Karatas, H. & Özden, S. (2004). *Acta Cryst.* E**60**, o1535–o1537.
Babadbani, B. M. & Mousavi, M. (2013). *Chemometrics & Intelligent Lab. Syst.* **122**, 1–11.
Becke, A. D. (1993). *J. Chem. Phys.* **98**, 5648–5652.
Bouayad, K., Kandri Rodi, Y., Elmsellem, H., El Ghadraoui, E. H., Ouzidan, Y., Abdel-Rahman, I., Kusuma, H. S., Warad, I., Mague, J. T., Essassi, E. M., Hammouti, B. & Chetouani, A. (2018). *Mor. J. Chem.* **6**, 22–34.
Brandenburg, K. & Putz, H. (2012). *DIAMOND*, Crystal Impact GbR, Bonn, Germany.
Bruker (2016). *APEX3* and *SAINT*. Bruker AXS Inc., Madison, Wisconsin, USA.
Burlov, A. S., Koshchienko, Y. V., Kiskin, M. A., Nikolaevskii, S. A., Garnovskii, D. A., Lermontov, A. S., Makarova, N. I., Metelitsa, A. V. & Eremenko, I. L. (2016). *J. Mol. Struct.* **1104**, 7–13.
Chanda, K., Maiti, B., Tseng, C.-C. & Sun, C.-M. (2012). *ACS Comb. Sci.* **14**, 115–123.
Cheng, Z., Zhang, Y. & Zhang, W. (2010). *Med. Chem. Res.* **19**, 1307–1325.
Devi, N., Jana, A. K. & Singh, V. (2018). *Karbala Int. J. Modern Sci.* 1–7.
Dymińska, L. (2015). *Bioorg. Med. Chem.* **23**, 6087–6099.
Ehmke, V., Winkler, E. W., Banner, D., Haap, W., Schweizer, W. B., Rottmann, M., Kaiser, M., Freymond, C., Schirmeister, T. & Diederich, F. (2013). *ChemMedChem*, **8**, 967–975.
El Kazzouli, S., Griffon du Bellay, A., Berteina-Raboin, S., Delagrange, P., Caignard, D. H. & Guillaumet, G. (2011). *Eur. J. Med. Chem.* **46**, 4252–4257.
Frisch, M. J., Trucks, G. W., Schlegel, H. B., Scuseria, G. E., Robb, M. A., Cheeseman, J. R., Scalmani, G., Barone, V., Mennucci, B., Petersson, G. A., Nakatsuji, H., Caricato, M., Li, X., Hratchian, H. P., Izmaylov, A. F., Bloino, J., Zheng, G., Sonnenberg, J. L., Hada, M., Ehara, M., Toyota, K., Fukuda, R., Hasegawa, J., Ishida, M., Nakajima, T., Honda, Y., Kitao, O., Nakai, H., Vreven, T., Montgomery, J. A., Jr., Peralta, J. E., Ogliaro, F., Bearpark, M., Heyd, J. J., Brothers, E., Kudin, K. N., Staroverov, V. N., Kobayashi, R., Normand, J., Raghavachari, K., Rendell, A., Burant, J. C., Iyengar, S. S., Tomasi, J., Cossi, M., Rega, N., Millam, J. M., Klene, M., Knox, J. E., Cross, J. B., Bakken, V., Adamo, C., Jaramillo, J., Gomperts, R., Stratmann, R. E., Yazyev, O., Austin, A. J., Cammi, R., Pomelli, C., Ochterski, J. W., Martin, R. L., Morokuma, K., Zakrzewski, V. G., Voth, G. A., Salvador, P., Dannenberg, J. J., Dapprich, S., Daniels, A. D., Farkas, Ö., Foresman, J. B., Ortiz, J. V., Cioslowski, J. & Fox, D. J. (2009). *GAUSSIAN09*. Gaussian Inc., Wallingford, CT, US.
Groom, C. R., Bruno, I. J., Lightfoot, M. P. & Ward, S. C. (2016). *Acta Cryst.* B**72**, 171–179.
Hathwar, V. R., Sist, M., Jørgensen, M. R. V., Mamakhel, A. H., Wang, X., Hoffmann, C. M., Sugimoto, K., Overgaard, J. & Iversen, B. B. (2015). *IUCrJ*, **2**, 563–574.
Hirshfeld, H. L. (1977). *Theor. Chim. Acta*, **44**, 129–138.
Kazak, C., Yilmaz, V. T., Goker, H. & Kus, C. (2006). *Cryst. Res. Technol.* **41**, 528–532.
Krause, L., Herbst-Irmer, R., Sheldrick, G. M. & Stalke, D. (2015). *J. Appl. Cryst.* **48**, 3–10.
Martínez-Urbina, M. A., Zentella, A., Vilchis-Reyes, M. A., Guzmán, A., Vargas, O., Ramírez Apan, M. T., Ventura Gallegos, J. L. & Díaz, E. (2010). *Eur. J. Med. Chem.* **45**, 1211–1219.
McKinnon, J. J., Jayatilaka, D. & Spackman, M. A. (2007). *Chem. Commun.* pp. 3814–3816.
Sheldrick, G. M. (2015*a*). *Acta Cryst.* A**71**, 3–8.
Sheldrick, G. M. (2015*b*). *Acta Cryst.* C**71**, 3–8.
Sikine, M., Elmsellem, H., Kandri Rodi, Y., Steli, H., Aouniti, A., Hammouti, B., Ouzidan, Y., Ouazzani Chahdi, F., Bourass, M. & Essassi, E. M. (2016). *J. Mater. Environ. Sci.* **7**, 4620–4632.
Spackman, M. A. & Jayatilaka, D. (2009). *CrystEngComm*, **11**, 19–32.
Tobo, A., Tobo, M., Nakakura, T., Ebara, M., Tomura, H., Mogi, C., Im, D., Murata, N., Kuwabara, A., Ito, S., Fukuda, H., Arisawa, M.,

Shuto, S., Nakaya, M., Kurose, H., Sato, K. & Okajima, F. (2015). *PLoS One*, **10**, e0129334.
Turner, M. J., McKinnon, J. J., Wolff, S. K., Grimwood, D. J., Spackman, P. R., Jayatilaka, D. & Spackman, M. A. (2017). *CrystalExplorer17*. The University of Western Australia.
Venkatesan, P., Thamotharan, S., Ilangovan, A., Liang, H. & Sundius, T. (2016). *Spectrochim. Acta A*, **153**, 625–636.
Westrip, S. P. (2010). *J. Appl. Cryst.* **43**, 920–925.
Yadav, M., Behera, D. & Kumar, S. (2014). *Surf. Interface Anal.* **46**, 640–652.
Zhang, T., Zhang, R., Zhao, Y. & Ni, Z. (2018). *Dyes Pigments*, **148**, 276–285.
Zhao, Y.-L., Yu, T.-Z. & Meng, J. (2009). *Acta Cryst.* E**65**, o3076.

supporting information

Acta Cryst. (2020). E**76**, 677-682 [https://doi.org/10.1107/S2056989020005228]

Crystal structure, Hirshfeld surface analysis and DFT studies of 6-bromo-3-(12-bromododecyl)-2-(4-nitrophenyl)-4*H*-imidazo[4,5-*b*]pyridine

Zainab Jabri, Karim Jarmoni, Tuncer Hökelek, Joel T. Mague, Safia Sabir, Youssef Kandri Rodi and Khalid Misbahi

Computing details

Data collection: *APEX3* (Bruker, 2016); cell refinement: *SAINT* (Bruker, 2016); data reduction: *SAINT* (Bruker, 2016); program(s) used to solve structure: *SHELXT* (Sheldrick, 2015*a*); program(s) used to refine structure: *SHELXL2018/1* (Sheldrick, 2015*b*); molecular graphics: *DIAMOND* (Brandenburg & Putz, 2012); software used to prepare material for publication: *publCIF* (Westrip, 2010).

6-Bromo-3-(12-bromododecyl)-2-(4-nitrophenyl)-3*H*-imidazo[4,5-*b*]pyridine

Crystal data

$C_{24}H_{30}Br_2N_4O_2$
M_r = 566.34
Triclinic, $P\overline{1}$
a = 6.3291 (11) Å
b = 9.8911 (17) Å
c = 21.133 (4) Å
α = 76.480 (2)°
β = 84.965 (3)°
γ = 73.891 (2)°
V = 1235.4 (4) Å^3
Z = 2
$F(000)$ = 576
D_x = 1.522 Mg m^{-3}
Mo $K\alpha$ radiation, λ = 0.71073 Å
Cell parameters from 9900 reflections
θ = 2.2–29.0°
μ = 3.31 mm^{-1}
T = 150 K
Column, light orange
0.48 × 0.23 × 0.20 mm

Data collection

Bruker SMART APEX CCD diffractometer
Radiation source: fine-focus sealed tube
Graphite monochromator
Detector resolution: 8.3333 pixels mm^{-1}
φ and ω scans
Absorption correction: multi-scan (*SADABS*; Krause *et al.*, 2015)
T_{min} = 0.23, T_{max} = 0.56
24139 measured reflections
6598 independent reflections
5337 reflections with $I > 2\sigma(I)$
R_{int} = 0.040
θ_{max} = 29.3°, θ_{min} = 2.0°
h = −8→8
k = −13→13
l = −29→29

Refinement

Refinement on F^2
Least-squares matrix: full
$R[F^2 > 2\sigma(F^2)]$ = 0.035
$wR(F^2)$ = 0.095
S = 1.03
6598 reflections
293 parameters
0 restraints
Primary atom site location: dual
Secondary atom site location: difference Fourier map

Hydrogen site location: inferred from neighbouring sites
H-atom parameters constrained

$w = 1/[\sigma^2(F_o^2) + (0.0494P)^2 + 0.370P]$ where $P = (F_o^2 + 2F_c^2)/3$
$(\Delta/\sigma)_{max} = 0.002$
$\Delta\rho_{max} = 0.72$ e Å^{-3}
$\Delta\rho_{min} = -0.80$ e Å^{-3}

Special details

Experimental. The diffraction data were obtained from 3 sets of 400 frames, each of width 0.5° in ω, colllected at φ = 0.00, 90.00 and 180.00° and 2 sets of 800 frames, each of width 0.45° in φ, collected at ω = -30.00 and 210.00°. The scan time was 10 sec/frame.

Geometry. All esds (except the esd in the dihedral angle between two l.s. planes) are estimated using the full covariance matrix. The cell esds are taken into account individually in the estimation of esds in distances, angles and torsion angles; correlations between esds in cell parameters are only used when they are defined by crystal symmetry. An approximate (isotropic) treatment of cell esds is used for estimating esds involving l.s. planes.

Refinement. Refinement of F^2 against ALL reflections. The weighted R-factor wR and goodness of fit S are based on F^2, conventional R-factors R are based on F, with F set to zero for negative F^2. The threshold expression of $F^2 > 2$sigma(F^2) is used only for calculating R-factors(gt) etc. and is not relevant to the choice of reflections for refinement. R-factors based on F^2 are statistically about twice as large as those based on F, and R- factors based on ALL data will be even larger. H-atoms attached to carbon were placed in calculated positions (C—H = 0.95 - 0.99 Å). All were included as riding contributions with isotropic displacement parameters 1.2 - 1.5 times those of the attached atoms. Br2 is disordered over two sites in a 0.902 (3)/0.098 (32) ratio with the two components refined with restraints that they have comparable geometries.

Fractional atomic coordinates and isotropic or equivalent isotropic displacement parameters (Å²)

	x	*y*	*z*	U_{iso}*/U_{eq}	Occ. (<1)
Br1	1.82823 (3)	0.88087 (2)	0.00828 (2)	0.02928 (7)	
Br2	−0.34993 (9)	0.51084 (14)	0.63610 (3)	0.05439 (19)	0.902 (3)
Br2A	−0.3773 (9)	0.5733 (11)	0.6273 (3)	0.05439 (19)	0.098 (3)
O1	0.4691 (3)	0.16270 (19)	0.13274 (10)	0.0470 (4)	
O2	0.3734 (3)	0.2314 (2)	0.22339 (9)	0.0468 (4)	
N1	1.3755 (3)	0.79656 (18)	0.15128 (8)	0.0244 (3)	
N2	1.1281 (3)	0.64593 (18)	0.16156 (8)	0.0239 (3)	
N3	1.2508 (3)	0.55633 (18)	0.06847 (8)	0.0234 (3)	
N4	0.4845 (3)	0.23168 (19)	0.17246 (10)	0.0317 (4)	
C1	1.3664 (3)	0.6514 (2)	0.07409 (9)	0.0222 (4)	
C2	1.5326 (3)	0.6991 (2)	0.03550 (10)	0.0241 (4)	
H2	1.588946	0.665956	−0.002911	0.029*	
C3	1.6108 (3)	0.7989 (2)	0.05705 (10)	0.0241 (4)	
C4	1.5370 (3)	0.8446 (2)	0.11371 (10)	0.0250 (4)	
H4	1.599544	0.910484	0.126734	0.030*	
C5	1.2880 (3)	0.7032 (2)	0.13151 (9)	0.0223 (4)	
C6	1.1134 (3)	0.5596 (2)	0.12076 (9)	0.0225 (4)	
C7	0.9500 (3)	0.4757 (2)	0.13404 (9)	0.0223 (4)	
C8	0.9326 (3)	0.3904 (2)	0.09185 (10)	0.0256 (4)	
H8	1.027479	0.386290	0.054538	0.031*	
C9	0.7781 (3)	0.3117 (2)	0.10385 (10)	0.0266 (4)	
H9	0.764906	0.253965	0.074998	0.032*	
C10	0.6431 (3)	0.3189 (2)	0.15897 (10)	0.0249 (4)	
C11	0.6535 (3)	0.4038 (2)	0.20136 (10)	0.0272 (4)	

H11	0.557276	0.407835	0.238384	0.033*	
C12	0.8083 (3)	0.4831 (2)	0.18856 (10)	0.0254 (4)	
H12	0.817963	0.542629	0.216954	0.031*	
C13	1.2921 (3)	0.8451 (2)	0.21174 (10)	0.0277 (4)	
H13A	1.407583	0.875235	0.229259	0.033*	
H13B	1.259112	0.763605	0.244503	0.033*	
C14	1.0856 (4)	0.9702 (2)	0.20091 (10)	0.0303 (4)	
H14A	0.979474	0.946902	0.176234	0.036*	
H14B	1.124005	1.057448	0.174668	0.036*	
C15	0.9786 (4)	1.0010 (2)	0.26569 (11)	0.0354 (5)	
H15A	1.093787	1.003377	0.293931	0.042*	
H15B	0.872569	1.097574	0.257308	0.042*	
C16	0.8594 (4)	0.8905 (3)	0.30167 (12)	0.0422 (6)	
H16A	0.766800	0.873698	0.270434	0.051*	
H16B	0.970288	0.798211	0.317524	0.051*	
C17	0.7154 (5)	0.9319 (3)	0.35888 (13)	0.0481 (7)	
H17A	0.608784	1.026430	0.343710	0.058*	
H17B	0.808726	0.943166	0.391508	0.058*	
C18	0.5895 (5)	0.8219 (3)	0.39151 (13)	0.0498 (7)	
H18A	0.499382	0.809373	0.358399	0.060*	
H18B	0.697061	0.727992	0.407038	0.060*	
C19	0.4406 (5)	0.8604 (3)	0.44815 (14)	0.0551 (8)	
H19A	0.334976	0.955515	0.433229	0.066*	
H19B	0.530537	0.869341	0.482227	0.066*	
C20	0.3130 (5)	0.7502 (3)	0.47773 (13)	0.0511 (7)	
H20A	0.418487	0.653915	0.489418	0.061*	
H20B	0.215232	0.746721	0.444409	0.061*	
C21	0.1746 (5)	0.7810 (3)	0.53790 (14)	0.0504 (7)	
H21A	0.268887	0.794690	0.569570	0.060*	
H21B	0.057909	0.872000	0.525371	0.060*	
C22	0.0687 (5)	0.6614 (3)	0.57043 (12)	0.0434 (6)	
H22A	0.182702	0.568038	0.577361	0.052*	
H22B	−0.041627	0.656911	0.541078	0.052*	
C23	−0.0432 (5)	0.6828 (3)	0.63564 (12)	0.0434 (6)	
H23A	0.059462	0.705909	0.661635	0.052*	
H23B	−0.173900	0.766726	0.627551	0.052*	
C24	−0.1145 (4)	0.5542 (3)	0.67503 (11)	0.0404 (5)	0.902 (3)
H24A	−0.164784	0.571989	0.718783	0.049*	0.902 (3)
H24B	0.014190	0.468801	0.680713	0.049*	0.902 (3)
C24A	−0.1145 (4)	0.5542 (3)	0.67503 (11)	0.0404 (5)	0.098 (3)
H24C	−0.150774	0.561926	0.720811	0.049*	0.098 (3)
H24D	−0.001810	0.462587	0.673847	0.049*	0.098 (3)

Atomic displacement parameters (Å²)

	U^{11}	U^{22}	U^{33}	U^{12}	U^{13}	U^{23}
Br1	0.02318 (11)	0.02607 (11)	0.04000 (13)	−0.01178 (8)	0.00655 (8)	−0.00638 (8)
Br2	0.0548 (2)	0.0723 (6)	0.04320 (19)	−0.0293 (3)	−0.00326 (15)	−0.0109 (3)

Br2A	0.0548 (2)	0.0723 (6)	0.04320 (19)	−0.0293 (3)	−0.00326 (15)	−0.0109 (3)
O1	0.0496 (11)	0.0440 (10)	0.0645 (12)	−0.0309 (8)	0.0154 (9)	−0.0294 (9)
O2	0.0465 (10)	0.0549 (11)	0.0518 (11)	−0.0357 (9)	0.0175 (8)	−0.0171 (9)
N1	0.0216 (8)	0.0245 (8)	0.0304 (8)	−0.0099 (6)	0.0014 (7)	−0.0087 (7)
N2	0.0224 (8)	0.0255 (8)	0.0276 (8)	−0.0119 (7)	0.0019 (6)	−0.0073 (7)
N3	0.0196 (8)	0.0236 (8)	0.0301 (8)	−0.0089 (6)	0.0003 (6)	−0.0082 (7)
N4	0.0279 (9)	0.0267 (9)	0.0437 (11)	−0.0140 (7)	0.0035 (8)	−0.0074 (8)
C1	0.0182 (9)	0.0219 (9)	0.0274 (9)	−0.0062 (7)	−0.0007 (7)	−0.0063 (7)
C2	0.0187 (9)	0.0224 (9)	0.0306 (10)	−0.0058 (7)	0.0013 (7)	−0.0053 (8)
C3	0.0170 (9)	0.0210 (9)	0.0334 (10)	−0.0066 (7)	0.0015 (7)	−0.0033 (8)
C4	0.0216 (9)	0.0211 (9)	0.0344 (10)	−0.0091 (7)	−0.0002 (8)	−0.0066 (8)
C5	0.0202 (9)	0.0219 (9)	0.0266 (9)	−0.0080 (7)	−0.0005 (7)	−0.0059 (7)
C6	0.0194 (9)	0.0228 (9)	0.0263 (9)	−0.0072 (7)	−0.0020 (7)	−0.0049 (7)
C7	0.0188 (9)	0.0211 (9)	0.0274 (9)	−0.0065 (7)	−0.0014 (7)	−0.0044 (7)
C8	0.0218 (9)	0.0252 (9)	0.0322 (10)	−0.0091 (8)	0.0033 (8)	−0.0088 (8)
C9	0.0232 (10)	0.0243 (9)	0.0366 (11)	−0.0095 (8)	0.0006 (8)	−0.0114 (8)
C10	0.0207 (9)	0.0214 (9)	0.0340 (10)	−0.0098 (7)	0.0004 (8)	−0.0039 (8)
C11	0.0231 (10)	0.0302 (10)	0.0292 (10)	−0.0108 (8)	0.0020 (8)	−0.0050 (8)
C12	0.0245 (10)	0.0275 (10)	0.0274 (10)	−0.0109 (8)	−0.0010 (8)	−0.0070 (8)
C13	0.0288 (11)	0.0302 (10)	0.0292 (10)	−0.0116 (8)	0.0019 (8)	−0.0129 (8)
C14	0.0322 (11)	0.0288 (10)	0.0312 (10)	−0.0111 (9)	0.0041 (8)	−0.0073 (9)
C15	0.0383 (13)	0.0298 (11)	0.0386 (12)	−0.0096 (9)	0.0092 (10)	−0.0117 (9)
C16	0.0457 (14)	0.0465 (14)	0.0412 (13)	−0.0219 (12)	0.0138 (11)	−0.0168 (11)
C17	0.0528 (16)	0.0397 (14)	0.0486 (15)	−0.0129 (12)	0.0184 (12)	−0.0102 (11)
C18	0.0584 (17)	0.0536 (16)	0.0413 (14)	−0.0229 (14)	0.0172 (12)	−0.0148 (12)
C19	0.0665 (19)	0.0431 (15)	0.0488 (15)	−0.0142 (13)	0.0258 (14)	−0.0070 (12)
C20	0.0589 (18)	0.0568 (17)	0.0365 (13)	−0.0198 (14)	0.0158 (12)	−0.0089 (12)
C21	0.0590 (17)	0.0378 (14)	0.0466 (15)	−0.0096 (12)	0.0208 (13)	−0.0058 (11)
C22	0.0490 (15)	0.0473 (14)	0.0335 (12)	−0.0146 (12)	0.0101 (11)	−0.0101 (11)
C23	0.0486 (15)	0.0449 (14)	0.0370 (12)	−0.0135 (12)	0.0122 (11)	−0.0129 (11)
C24	0.0434 (14)	0.0483 (14)	0.0307 (11)	−0.0158 (11)	0.0009 (10)	−0.0069 (10)
C24A	0.0434 (14)	0.0483 (14)	0.0307 (11)	−0.0158 (11)	0.0009 (10)	−0.0069 (10)

Geometric parameters (Å, º)

Br1—C3	1.8954 (19)	C14—H14A	0.9900
Br2—C24	1.953 (3)	C14—H14B	0.9900
Br2A—C24A	1.962 (5)	C15—C16	1.520 (3)
O1—N4	1.224 (2)	C15—H15A	0.9900
O2—N4	1.233 (2)	C15—H15B	0.9900
N1—C5	1.357 (2)	C16—C17	1.514 (3)
N1—C4	1.361 (2)	C16—H16A	0.9900
N1—C13	1.473 (3)	C16—H16B	0.9900
N2—C5	1.336 (2)	C17—C18	1.526 (4)
N2—C6	1.372 (3)	C17—H17A	0.9900
N3—C6	1.346 (2)	C17—H17B	0.9900
N3—C1	1.372 (2)	C18—C19	1.511 (4)
N4—C10	1.465 (2)	C18—H18A	0.9900

C1—C2	1.392 (3)	C18—H18B	0.9900
C1—C5	1.423 (3)	C19—C20	1.520 (4)
C2—C3	1.396 (3)	C19—H19A	0.9900
C2—H2	0.9500	C19—H19B	0.9900
C3—C4	1.376 (3)	C20—C21	1.521 (4)
C4—H4	0.9500	C20—H20A	0.9900
C6—C7	1.467 (3)	C20—H20B	0.9900
C7—C8	1.393 (3)	C21—C22	1.517 (4)
C7—C12	1.400 (3)	C21—H21A	0.9900
C8—C9	1.383 (3)	C21—H21B	0.9900
C8—H8	0.9500	C22—C23	1.526 (3)
C9—C10	1.387 (3)	C22—H22A	0.9900
C9—H9	0.9500	C22—H22B	0.9900
C10—C11	1.380 (3)	C23—C24A	1.507 (3)
C11—C12	1.389 (3)	C23—C24	1.507 (3)
C11—H11	0.9500	C23—H23A	0.9900
C12—H12	0.9500	C23—H23B	0.9900
C13—C14	1.521 (3)	C24—H24A	0.9900
C13—H13A	0.9900	C24—H24B	0.9900
C13—H13B	0.9900	C24A—H24C	0.9900
C14—C15	1.531 (3)	C24A—H24D	0.9900

C5—N1—C4	118.57 (17)	C17—C16—C15	115.0 (2)
C5—N1—C13	119.67 (16)	C17—C16—H16A	108.5
C4—N1—C13	121.75 (17)	C15—C16—H16A	108.5
C5—N2—C6	100.79 (16)	C17—C16—H16B	108.5
C6—N3—C1	102.17 (16)	C15—C16—H16B	108.5
O1—N4—O2	123.30 (19)	H16A—C16—H16B	107.5
O1—N4—C10	118.48 (18)	C16—C17—C18	113.4 (2)
O2—N4—C10	118.22 (18)	C16—C17—H17A	108.9
N3—C1—C2	132.04 (18)	C18—C17—H17A	108.9
N3—C1—C5	107.59 (16)	C16—C17—H17B	108.9
C2—C1—C5	120.37 (18)	C18—C17—H17B	108.9
C1—C2—C3	115.51 (18)	H17A—C17—H17B	107.7
C1—C2—H2	122.2	C19—C18—C17	115.1 (2)
C3—C2—H2	122.2	C19—C18—H18A	108.5
C4—C3—C2	123.24 (18)	C17—C18—H18A	108.5
C4—C3—Br1	115.85 (15)	C19—C18—H18B	108.5
C2—C3—Br1	120.92 (15)	C17—C18—H18B	108.5
N1—C4—C3	120.73 (18)	H18A—C18—H18B	107.5
N1—C4—H4	119.6	C18—C19—C20	113.3 (3)
C3—C4—H4	119.6	C18—C19—H19A	108.9
N2—C5—N1	126.94 (18)	C20—C19—H19A	108.9
N2—C5—C1	111.52 (17)	C18—C19—H19B	108.9
N1—C5—C1	121.53 (17)	C20—C19—H19B	108.9
N3—C6—N2	117.92 (17)	H19A—C19—H19B	107.7
N3—C6—C7	121.76 (17)	C19—C20—C21	114.2 (3)
N2—C6—C7	120.31 (17)	C19—C20—H20A	108.7

C8—C7—C12	119.67 (18)	C21—C20—H20A	108.7
C8—C7—C6	120.18 (18)	C19—C20—H20B	108.7
C12—C7—C6	120.14 (18)	C21—C20—H20B	108.7
C9—C8—C7	120.52 (19)	H20A—C20—H20B	107.6
C9—C8—H8	119.7	C22—C21—C20	113.0 (2)
C7—C8—H8	119.7	C22—C21—H21A	109.0
C8—C9—C10	118.46 (19)	C20—C21—H21A	109.0
C8—C9—H9	120.8	C22—C21—H21B	109.0
C10—C9—H9	120.8	C20—C21—H21B	109.0
C11—C10—C9	122.63 (18)	H21A—C21—H21B	107.8
C11—C10—N4	119.21 (18)	C21—C22—C23	112.7 (2)
C9—C10—N4	118.16 (18)	C21—C22—H22A	109.0
C10—C11—C12	118.37 (19)	C23—C22—H22A	109.0
C10—C11—H11	120.8	C21—C22—H22B	109.0
C12—C11—H11	120.8	C23—C22—H22B	109.0
C11—C12—C7	120.34 (19)	H22A—C22—H22B	107.8
C11—C12—H12	119.8	C24A—C23—C22	114.3 (2)
C7—C12—H12	119.8	C24—C23—C22	114.3 (2)
N1—C13—C14	112.14 (17)	C24—C23—H23A	108.7
N1—C13—H13A	109.2	C22—C23—H23A	108.7
C14—C13—H13A	109.2	C24—C23—H23B	108.7
N1—C13—H13B	109.2	C22—C23—H23B	108.7
C14—C13—H13B	109.2	H23A—C23—H23B	107.6
H13A—C13—H13B	107.9	C23—C24—Br2	114.01 (18)
C13—C14—C15	111.20 (18)	C23—C24—H24A	108.8
C13—C14—H14A	109.4	Br2—C24—H24A	108.8
C15—C14—H14A	109.4	C23—C24—H24B	108.8
C13—C14—H14B	109.4	Br2—C24—H24B	108.8
C15—C14—H14B	109.4	H24A—C24—H24B	107.6
H14A—C14—H14B	108.0	C23—C24A—Br2A	99.5 (3)
C16—C15—C14	113.51 (19)	C23—C24A—H24C	111.9
C16—C15—H15A	108.9	Br2A—C24A—H24C	111.9
C14—C15—H15A	108.9	C23—C24A—H24D	111.9
C16—C15—H15B	108.9	Br2A—C24A—H24D	111.9
C14—C15—H15B	108.9	H24C—C24A—H24D	109.6
H15A—C15—H15B	107.7		

C6—N3—C1—C2	−179.2 (2)	C6—C7—C8—C9	−179.63 (18)
C6—N3—C1—C5	0.9 (2)	C7—C8—C9—C10	−0.5 (3)
N3—C1—C2—C3	179.6 (2)	C8—C9—C10—C11	1.5 (3)
C5—C1—C2—C3	−0.4 (3)	C8—C9—C10—N4	−178.13 (18)
C1—C2—C3—C4	2.3 (3)	O1—N4—C10—C11	176.3 (2)
C1—C2—C3—Br1	−177.37 (13)	O2—N4—C10—C11	−3.8 (3)
C5—N1—C4—C3	−0.3 (3)	O1—N4—C10—C9	−4.1 (3)
C13—N1—C4—C3	−179.31 (18)	O2—N4—C10—C9	175.81 (19)
C2—C3—C4—N1	−2.0 (3)	C9—C10—C11—C12	−1.0 (3)
Br1—C3—C4—N1	177.68 (14)	N4—C10—C11—C12	178.54 (18)
C6—N2—C5—N1	−178.66 (19)	C10—C11—C12—C7	−0.3 (3)

C6—N2—C5—C1	−0.1 (2)	C8—C7—C12—C11	1.2 (3)
C4—N1—C5—N2	−179.38 (18)	C6—C7—C12—C11	−179.94 (18)
C13—N1—C5—N2	−0.4 (3)	C5—N1—C13—C14	−83.3 (2)
C4—N1—C5—C1	2.2 (3)	C4—N1—C13—C14	95.7 (2)
C13—N1—C5—C1	−178.80 (18)	N1—C13—C14—C15	169.76 (17)
N3—C1—C5—N2	−0.5 (2)	C13—C14—C15—C16	−74.4 (3)
C2—C1—C5—N2	179.53 (17)	C14—C15—C16—C17	−168.7 (2)
N3—C1—C5—N1	178.14 (17)	C15—C16—C17—C18	177.0 (2)
C2—C1—C5—N1	−1.8 (3)	C16—C17—C18—C19	−179.0 (3)
C1—N3—C6—N2	−1.0 (2)	C17—C18—C19—C20	178.2 (3)
C1—N3—C6—C7	178.18 (17)	C18—C19—C20—C21	175.8 (3)
C5—N2—C6—N3	0.7 (2)	C19—C20—C21—C22	−173.9 (3)
C5—N2—C6—C7	−178.50 (17)	C20—C21—C22—C23	172.0 (3)
N3—C6—C7—C8	−0.5 (3)	C21—C22—C23—C24A	−169.6 (2)
N2—C6—C7—C8	178.74 (18)	C21—C22—C23—C24	−169.6 (2)
N3—C6—C7—C12	−179.32 (18)	C22—C23—C24—Br2	−66.7 (3)
N2—C6—C7—C12	−0.1 (3)	C22—C23—C24A—Br2A	−76.3 (3)
C12—C7—C8—C9	−0.8 (3)		

Hydrogen-bond geometry (Å, º)

D—H···*A*	*D*—H	H···*A*	*D*···*A*	*D*—H···*A*
C4—H4···O1^{i}	0.95	2.43	3.171 (3)	135
C24—H24*A*···O2^{ii}	0.99	2.53	3.372 (3)	142

Symmetry codes: (i) *x*+1, *y*+1, *z*; (ii) −*x*, −*y*+1, −*z*+1.